Published in final edited form as:
Nucl Med Biol. 2010 May ; 37(4): 479–486. doi:10.1016/j.nucmedbio.2010.01.006.

Comparison of the SERT-selective [^{18}F]FPBM and VMAT2-selective [^{18}F]AV-133 radiotracers in a rat model of Parkinson's Disease

Julie L. Wang[1], **Shunichi Oya**[2], **Ajit K. Parhi**[2], **Brian P. Lieberman**[2], **Karl Ploessl**[2], **Catherine Hou**[2], and **Hank F. Kung**[1,2,*]

[1]Department of Pharmacology, University of Pennsylvania School of Medicine, Philadelphia, PA 19104

[2]Department of Radiology, University of Pennsylvania School of Medicine, Philadelphia, PA 19104

Abstract

Introduction—The utility of [^{18}F]FPBM (2-(2′-((dimethylamino)methyl)-4′-(3-[^{18}F]-fluoropropoxy)phenylthio)benzenamine), a selective serotonin transporter (SERT) tracer, and [^{18}F]AV-133 ((+)-2-Hydroxy-3-isobutyl-9-(3-fluoropropoxy)-10-methoxy-1,2,3,4,6,7-hexahydro-11bH-benzo[a]quinolizine), a selective vesicular monoamine transporter 2 (VMAT2) tracer, were tested in the 6-hydroxydopamine (6-OHDA) unilateral lesioned rat model.

Methods—PET imaging of three 6-OHDA unilateral lesioned male Sprague Dawley rats (rats #1-3) were performed with [^{18}F]FPBM and [^{18}F]AV-133 to examine whether changes in SERT and VMAT2 binding, respectively, could be detected in the brain. The brains of the three rats were then removed and examined by *in vitro* autoradiography with [^{18}F]FPBM and the dopamine transporter ligand, [^{125}I]IPT, for confirmation.

Results—PET image analysis showed varying levels of SERT binding reduction (rat #1 = −11%, rat #2 = −4%, rat #3 = −43%; n = 2) and a clear and definitive loss of VMAT2 binding (rat #1 = −87%, rat #2 = −72%, and rat #3 = −91%; n = 1) in the left striatum when compared to the right (non-lesioned side) striatum. The results from PET imaging were corroborated with quantitative *in vitro* autoradiography. Rats treated with a selective serotonin toxin (PCA, p-chloroamphetamine) showed a significant reduction of uptake in the cortex and hypothalamus regions of the brain.

Conclusion—The preliminary data suggest that [^{18}F]FPBM and [^{18}F]AV-133 may be useful for the examination of serotonergic and dopaminergic neuron integrity, respectively, in the living brain.

Keywords

brain imaging; radioligand; SERT; VMAT2; Parkinson's Disease

*Corresponding author contact information: 3700 Market Street, Suite 305 Departments of Radiology and Pharmacology University of Pennsylvania School of Medicine Philadelphia, PA 1910 Tel: (215) 662-3096, Fax: (215) 349-5035 kunghf@sunmac.spect.upenn.edu.

1. Introduction

The serotonin transporter (SERT) in the brain is a major target for drug therapy against depression as well as other psychiatric disorders [1-4]. Selective serotonin reuptake inhibitors (SSRIs), which bind to and inhibit the transporter [5], are regularly prescribed for the treatment of depression. SERT imaging may then be useful for monitoring antidepressant drug occupancy and in turn, optimizing drug therapy [6-8]. Furthermore, due to SERT's location on the serotoneric neuron, this transporter can be used as a marker for examining serotonergic neuron integrity. Thus, SERT imaging can be employed in the pathophysiological study of neurodegenerative diseases that involve the serotonergic system such as Alzheimer's and Parkinson's disease [9-12].

Though Parkinson's disease is mainly associated with the loss of dopaminergic neurons, changes in the serotonergic system have been reported as well. Human patients with Parkinson's disease exhibit a decrease in SERT binding in the striatum and other areas as shown through *in vivo* positron emission tomography (PET) and single photon emission computed tomography (SPECT) imaging studies with [^{11}C]DASB, [^{11}C](+)McN5652, and [^{123}I]ß-CIT [9,10,13,14]. Patients also display a loss of serotonin, serotonin metabolite (5-HIAA), and serotonergic neurons as determined through post-mortem studies [15,16]. If characteristic neurological changes are known, SERT imaging may be developed as a non-invasive, early diagnostic tool. Catching this, as of yet, incurable disease at an early stage would afford patients a window of time to acquire treatment aimed at slowing the progression of the disease.

Significant efforts have been made to develop a suitable ^{18}F labeled SERT radiotracer for PET [17-22], but there has been limited success in the past and currently there is still no such FDA approved radiotracer. Using the longer lived ^{18}F isotope ($t_{1/2}$ = 110 min) compared to the shorter lived ^{11}C isotope ($t_{1/2}$ = 20 min) would allow medical centers, lacking the necessary radiochemistry facilities for their own production of the radiotracer to have access to the radiotracer from off-site commercial sources. Recently, a new promising SERT radiotracer, [^{18}F]FPBM (Fig 1), has been shown to possess high affinity (K_i = 0.38 nM), good selectivity, high brain uptake (0.99 % dose/g at 2 min post-injection), and an excellent target to non-target ratio (7.7 at 120 min post-injection) through *in vitro* binding assays, *in vivo* biodistribution, ex vivo autoradiography, and PET imaging studies in normal rats [23-25]. This compound was also amenable to simple radiosynthesis with relatively good radiochemical yields, good specific activity, and high radiochemical purity [23-25]. With these promising results, further studies were performed with [^{18}F]FPBM in a rat model of Parkinson's disease induced by a 6-hydroxydopamine (6-OHDA) unilateral lesion of the nigrostriatal pathway. An additional selective serotonin neuron toxin, p-chloroamphetamine (PCA), treated rat model was also used to test the selectivity of [^{18}F]FPBM uptake in the rat brain.

The goal of this study was to determine whether using the new radiotracer, [^{18}F]-FPBM, could detect changes in SERT binding in an *in vivo* model of a disease known to involve the serotonergic system. The unilaterally lesioned Parkinson's rat model was chosen because in addition to the loss of dopaminergic innervation, immunohistochemical studies have shown that a reduction in striatal serotonin innervation also occurred in the lesioned side of young adult rats that were injected with 6-OHDA in the left nigrostriatal bundle [26]. Though it has been reported that an intraventricular or intracisternal 6-OHDA injection causes serotonergic hyperinnervation of the neostriatum, this was only seen in neonatal rats and not in adult rats [27-30]. Furthermore, this model was selected because it allows for comparison between a "disease" (left striatum) and control (right striatum) condition within the same animal.

Examination was focused on the striatum because it is a sufficiently large, paired region that allows for easy visualization through small animal PET.

In addition to these [^{18}F]FPBM studies, PET imaging studies with the vesicular monoamine transporter 2 (VMAT2)-selective ligand, [^{18}F]AV-133, were performed. [^{18}F]AV-133 has been previously characterized through *in vitro* binding assays using mouse striatal homogenates, *in vivo* biodistribution studies in normal mice and 6-OHDA unilaterally lesioned mice, ex vivo autoradiography in mice, and pharmacokinetic studies in rat and monkey brains [31-33]. In the brain, VMAT2 is often referred to as the "gold standard" of dopaminergic neuron markers [34]. This is due to the fact that, in the striatum, most VMAT2 are localized on dopaminergic nerve terminals and they are resistant to drug-compensatory regulation. [^{11}C]DTBZ is a commonly used VMAT2-selective ligand that has been used for examining dopaminergic neuron integrity. [^{18}F]AV-133 has also been evaluated as a VMAT2 radiotracer for beta-cell mass in the pancreas [35]. VMAT2 binding sites are highly expressed in the islets of Langerhans [36,37]. Thus, PET imaging with [^{18}F]AV-133 was used to confirm whether the 6-OHDA lesions in these rats were successful. At the same time, these imaging studies serve as a comparison of [^{18}F]AV-133 and [^{18}F]FPBM as ^{18}F labeled radiotracers for imaging the brain.

Reported herein are the results on comparison of studies of the SERT-selective [^{18}F]FPBM and VMAT2-selective [^{18}F]AV-133 radiotracers in a rat model of Parkinson's Disease.

2. Materials and Methods

2.1 General

Three young adult, male Sprague-Dawley rats (310-330 g) lesioned unilaterally in the nigrostriatal pathway (coordinates from Bregma: AP-4.3, ML +1.2, DV −8.3) with 6-OHDA were obtained commercially from Taconic Farms, Inc. (Hudson, NY). The company verified the success of the lesion by evaluating the rat's response to a subcutaneous injection of apomorphine (0.05 mg/kg) 21 days post-lesion. Only rats with a total of 180 rotations/30 min or multiple 5 min periods of ≥ 6 rotations/min were used. Rats were anesthetized by inhalation of 1.5-2.5% isoflurane during the length of PET imaging and prior to any injections and sacrifice. All protocols requiring the utilization of rats were reviewed and approved by the Institutional Animal Care and Use Committee (University of Pennsylvania).

[^{125}I]IPT (*N*-(3′-[^{125}I]-iodopropen-2′-yl)-2-beta-carbomethoxy-3-beta-(4-chloro phenyl) tropane) was prepared following the procedure described previously [38]. [^{18}F]AV-133 ((+)-2-Hydroxy-3-isobutyl-9-(3-[^{18}F]-fluoropropoxy)-10-methoxy1,2,3,4,6,7-hexahydro-11bH-benzo[a]quinolizine) synthesis procedures were reported previously [31] and was successfully prepared with a specific activity of 48-390 Gbq/ummol at the end of synthesis (EOS). The labeling and purification procedures of [^{18}F]FPBM (2-(2′-((dimethylamino)methyl)-4′-(3-^{18}F-fluoropropoxy)phenylthio)benzenamine) have also been reported previously [23], and [^{18}F]FPBM was obtained with a specific activity of 8-87 GBq/umol at EOS.

2.2 Small Animal PET Imaging

Imaging was performed using the Philips Mosaic Animal PET imaging system. SERT binding was examined by injecting 37-51 MBq of [^{18}F]FPBM via tail vein. Imaging commenced immediately after injection and continued for a period of 4 hrs taking 5 min per frame for the first 2 hrs and 15 min per frame for the last 2 hrs. Each rat was imaged a second time with [^{18}F]FPBM 7-20 days later. To examine VMAT2 binding in the rats, [^{18}F]AV-133 (50-57 MBq) was also injected via tail vein approximately 4 weeks later and imaged as above (n = 1). Normal control rats were also imaged with [^{18}F]FPBM (43-57

MBq) for comparison. Region-of-interest analysis was performed using AMIDE (http://amide.sourceforge.net/) on reconstructed images to generate time activity curves. Points from the same brain region were summed to obtain total activity in that region. The percent binding change between the left and right striatum was expressed as ((total activity in right striatum − total activity in cerebellum) − (total activity in left striatum − total activity in cerebellum))/(total activity in right striatum − total activity in cerebellum) × 100.

Analysis of the [^{18}F]FPBM time activity curves generated from PET image analysis (Fig 4) showed the normal control rat to have comparable binding in the left and right striatum (Fig 4A). For the control, PET imaging was done in two separate rats, and the average percent binding change in the left striatum was +0.5% (n = 2, +4.5 and −3.5%). For the 6-OHDA lesioned rats, each rat was scanned twice. Rat #1 (Fig 4B) had an average [^{18}F]FPBM binding reduction of −11% in the left striatum (n = 2, −12% and −10%, 10 days between scans). Rats #2 and #3 (Fig 4C-D) had average reductions of −4% (n = 2, −1% and −7%, 20 days between scans) and −43% (n = 2, −42% and −44%, 7 days between scans), respectively.

2.3 Preparation of ^{125}I Calibration Standards

Embedding medium (OCT, Sakura Tissue Tek®) was added to a tissue embedding mold, and micro test tubes (5 mm diameter) fixed in a homemade test tube rack were lowered into the medium. The medium was frozen, and the tubes were removed leaving behind wells. This well block was kept on powdered dry ice. ^{125}I labeled ligands no longer in use were compiled, dried down under an Argon (*g*) stream, and redissolved in 50% ethanol to a concentration of 0.2 MBq/μL. Evans blue was added to the mixed radioligand solution, and dilutions of the radioligand were made to give a range of ten concentrations. Homogenates were made from frozen rat brains (Pel-Freeze® Biologicals) using a Wheaton overhead stirrer. The radioligand (5 μL) was mixed into a 0.7 mL aliquot of brain homogenate using a spatula until the blue color was evenly distributed. The mixed homogenate was then transferred to a 3 mL needleless syringe, and the homogenate was injected into a well in the frozen well block. An aliquot of the homogenate mixture was also weighed and counted by gamma counter to determine the final concentration of the standard. This was done for all radioligand concentrations. Final concentrations ranged from 0.04-1.48 kBq/mg. The complete frozen well block was then sliced into 20 μm sections on a cryostat microtome and thaw-mounted on microscope slides.

The standards were exposed to film (Kodak BioMax MR) along with the brain sections used for *in vitro* autoradiography for 24 hrs. Image analysis was performed using ImageJ (http://rsb.info.nih.gov/ij/). To avoid inaccurate measurement due to small air bubbles in the standards, the mean gray values for five equal circular areas within each standard concentration (without air bubbles) were averaged. A calibration curve was generated with these averaged mean gray values and the known concentrations of the standards.

2.4 In vitro Autoradiography

The rats were decapitated and the brains were removed immediately. The brains were placed in OCT embedding medium and frozen with powdered dry ice. Coronal sections (20 μm) were sliced on a cryostat microtome and thaw-mounted on microscope slides. The slides were desiccated at 4 °C for 2 hrs and then stored at −70 °C. Prior to each experiment, sections were thawed, air-dried at room temperature, and preincubated for 20 min at room temperature with buffer containing 50 mM Tris and 120 mM NaCl (pH 7.4). Following preincubation, the sections were allowed to dry at room temperature. Each section was covered with 400 μL of preincubation buffer containing [^{18}F]FPBM (166-178 Bq/μL) for 1 hr at room temperature. The sections were rinsed with cold preincubation buffer in Coplin

jars for 2 × 45 min and then rinsed once quickly with cold H_2O. For [^{125}I]IPT (13-19 Bq/μL) labeling of neighboring sections, the same procedures were used with the following exceptions: buffer contained 50 mM Na_2HPO_4 and 0.32 M sucrose (pH 7.4), radioligand incubation was 2 hrs, and sections were rinsed for 2 × 30 min [38]. The sections were allowed to air-dry at room temperature and then exposed to film (Kodak BioMax MR) along with the ^{125}I standards for 24 hrs.

Films were scanned (Epson Expression 1600, 8-bit grayscale, 600 dpi), and image analysis was performed using ImageJ (http://rsb.info.nih.gov/ij/). The region of interest (striatum) was outlined according to the anatomical boundary defined in the Paxinos and Watson rat brain atlas. The percent binding change between the left and right striatum was expressed as ((right striatum − cerebellum) − (left striatum − cerebellum))/(right striatum − cerebellum) × 100. The percent binding change in the left striatum was determined for multiple brain sections that spanned from the rostral to caudal striatum, and brain sections were then averaged together.

2.5. p-chloroamphetamine (PCA) treatment of rats

A neurotoxin, p-chloroamphetamine (PCA), was used to lesion the serotonergic neurons of male Sprague Dawley rats, as described previously [39]. Twelve rats were divided into two groups, and were injected daily with PCA (5 mg/kg, i.p.) or saline for 2 consecutive days, respectively. Six days later, the rats were injected with [^{18}F]FPBM (~925 μBq, i.v.) and sacrificed by using isoflurane 60 minutes post injection. The biodistribution of [^{18}F]FPBM was measured in the control and PCA-lesioned rat brains only and no peripheral organs. PET imaging was not performed for PCA- treated rats.

3. Results

3.1 Small Animal PET Imaging

A summed PET image (4 hrs) for each of the three 6-OHDA lesioned rats (rats #1-3) after an injection of the VMAT2 ligand, [^{18}F]AV-133, are shown in Figure 2. Clear loss of [^{18}F]AV-133 binding can be seen in the left striatum for each of the rats (rat #1 = −87%, rat #2 = −72%, rat #3 = −91%, n = 1). This binding loss suggested that the dopaminergic neurons in the left striatum were successfully lesioned and that [^{18}F]AV-133 may be useful for imaging VMAT2 in the brain. Figure 3 shows SERT binding with [^{18}F]FPBM in a normal control rat and the same three lesioned rats. The normal control rat appeared to have similar [^{18}F]FPBM binding in the left and right striatum as expected (Fig 3A). Rat #1 had a slight reduction of activity in the left striatum (Fig 3B), rat #2 did not appear to show binding reduction (Fig 3C), and rat #3 showed an obvious loss of [^{18}F]FPBM binding (Fig 3D). Each 6-OHDA lesioned rat was then imaged a second time with [^{18}F]FPBM 7-20 days later, and the results were similar (images not shown). Localization of [^{18}F]FPBM to the SERT-rich region, the thalamus, can also be clearly visualized (Fig 3).

3.2 In vitro Autoradiography

In vitro autoradiography was performed to confirm the results seen through PET imaging. The DAT ligand, [^{125}I]IPT, showed similar levels of DAT binding in the left and right striatum of a normal control rat as expected (Fig 5A top row). [^{125}I]IPT binding was dramatically reduced in the left striatum of lesioned rats #1, 2, and 3 (Fig 5B top row, images for rat #1 and #2 not shown) implying a loss of dopaminergic neurons. On neighboring brain sections [^{18}F]FPBM showed similar levels of SERT binding in the left and right striatum of a normal control rat as anticipated (Fig 5A bottom row). In lesioned rat #3 [^{18}F]FPBM binding appeared to be reduced in the left striatum (Fig 5B bottom row, red

arrows); however, [^{18}F]FPBM binding loss was not visible in rat #1 or #2 (images not shown).

Quantitative analysis of the *in vitro* autoradiography images and comparison to the results from PET image analysis show a similar trend (Fig 6). *In vitro* autoradiography with [^{125}I]IPT showed a −66% change in binding for rat #1, −56% for rat #2, and −81% for rat #3 (Fig 6A). PET imaging with [^{18}F]AV-133 and *in vitro* autoradiography with [^{125}I]IPT together suggest that the 6-OHDA lesions resulted in the loss of dopaminergic neurons in rats #1-3. The data also indicate that rat #3 had the greatest loss of dopaminergic neurons followed by rat #1 and then rat #2. Quantitative *in vitro* autoradiography of serotonergic neurons using [^{18}F]FPBM showed a large variation in percent binding changes in the left striatum between brain sections. However, averaged values for brain sections containing the rostral striatum (n = 2 for control rat, n = 3 for rats #1-3) ranked the lesioned rats in the same order of SERT binding loss as PET imaging with [^{18}F]FPBM, rat #3 > rat #1 > rat #2 (Fig 6B).

3.3 Changes in SERT Binding after Treatment of p-Chloro-Amphetamine (PCA)

As expected, the p-chloroamphetamine (PCA) treatment significantly reduced the binding of [^{18}F]FPBM in the hypothalamus of rat brain, a region where serotonin transporters are concentrated. The reduction was 52 and 68% in the hypothalamus and cortex, respectively (Table 1). The reduction of absolute uptake values in the cortex and hypothalamus are consistent with those reported previously using [^{11}C]DASB as the ligand in the same PCA lesioned rat model [40]. The data strongly supports the conclusion that binding of the new ligand, [^{18}F]FPBM, in the brain is associated with SERT binding sites.

4. Discussion

Through PET imaging in a rat model of Parkinson's disease, it was shown that [^{18}F]FPBM and [^{18}F]AV-133 can be used for the *in vivo* examination of SERT and VMAT2, respectively, in a "diseased" brain. Results from SERT imaging with [^{18}F]FPBM suggested that rat #3 had the greatest reduction of serotonergic innervation in the left striatum just as results from VMAT2 imaging with [^{18}F]AV-133 suggested that rat #3 had the greatest reduction of dopaminergic innervation in the left striatum. Imaging of both targets also suggested that rat #2 had the least amount of serotonergic and dopaminergic loss.

In vitro autoradiography with [^{18}F]FPBM was performed with the goal of confirming the results seen through PET imaging with [^{18}F]FPBM. The quantified values obtained from the [^{18}F]FPBM autoradiography images of individual brain sections fluctuated, but averaged values did reflect the results from PET imaging with [^{18}F]FPBM. Averaged percent binding reduction of the left rostral striatum brain sections for rat #1-3 (n = 3) were −5.9%, +2.3%, and −37.3%, respectively (Fig 6B). Only rostral striatum sections were averaged because it was observed in rat #3 that as the brain sections progressed to the caudal striatum, less binding reduction was seen in the left striatum. If brain sections containing the rostral through caudal striatum for rat #3 were averaged together, the average percent reduction would have been −22.2% (n = 8). Since only minor binding changes in the rostral striatum were seen for rat #1 and #2, averaging all striatum sections did not appreciably alter the results for rat #1 and #2 (+3.3%, n = 9 and +0.8%, n = 6, respectively).

A possible explanation for the fluctuation in values seen between brain sections may be due to different degrees of serotonergic neuron loss in various subregions of the striatum [26]. Another possible explanation may be that this autoradiographic method is less robust for SERT detection than for DAT detection since there is a lower density of serotonergic neurons in the striatum than dopaminergic neurons [41]. Subtracting cerebellum counts from

already relatively low striatum counts would greatly affect the calculated percent binding change. Working with an ^{18}F labeled ligand would also produce images that are less refined on autoradiographic film due to the nature of the isotope's radioactive decay of producing fewer Auger electrons. Moreover, incubation and rinsing conditions for the brain sections could have been optimized further.

Results from *in vitro* autoradiography with [^{18}F]FPBM correlated with results from [^{18}F]FPBM PET imaging, and results from *in vitro* autoradiography with [^{125}I]IPT, a dopamine transporter-selective ligand, correlated with results from [^{18}F]AV-133 PET imaging. Moreover, the rank of implied serotonergic neuron loss between the three rats follow the same rank of implied dopaminergic neuron loss (rat #3 > rat #1 > rat #2). The combination of preliminary evidence reported in this paper suggest that [^{18}F]FPBM may be useful for detecting changes in serotonergic innervation, and [^{18}F]AV-133 may be useful for detecting changes in dopaminergic innervation in the brain. However, additional studies with a larger sample population are warranted to determine the changes of SERT binding sites in the brain.

5. Conclusions

The 6-hydroxydopamine unilateral lesion of the nigrostriatal pathway is a common rat model of Parkinson's disease. PET imaging with [^{18}F]FPBM was successful in detecting a reduction of SERT binding, and [^{18}F]AV-133 was successful in detecting the loss of VMAT2 binding in the striatum (lesioned side) of these Parkinson's model rats. The results lend support that [^{18}F]FPBM can be used for detecting serotonergic neuron loss, and [^{18}F]AV-133 can be used for detecting dopaminergic neuron loss in the living brain. [^{18}F]FPBM and [^{18}F]AV-133 may thus serve as useful tools in the diagnosis and treatment of diseases involving the serotonergic and dopaminergic system, respectively.

Acknowledgments

This work was supported by the National Institutes of Health (Grant R01-MH068782, H.F.K.). PET imaging was performed at the Small Animal Imaging Facility (SAIF) at the University of Pennsylvania. The authors gratefully thank Eric Blankemeyer of SAIF for his technical expertise and Ms. Alex Paine for her editorial assistance.

Financial support: This work was supported by a grant awarded from the National Institutes of Health (ROI-MH068782, H.F.K.).

Abbreviations

5-HIAA	5-hydroxyindoleacetic acid
6-OHDA	6-hydroxydopamine
ß-CIT	(−)-2β-Carbomethoxy-3β-(4-iodophenyl)tropane
Am	amygdala
AV-133	(+)-2-Hydroxy-3-isobutyl-9-(3-fluoropropoxy)-10-methoxy-1,2,3,4,6,7-hexahydro-11bH-benzo[a]quinolizine
Cb	cerebellum
DASB	(N,N-dimethyl-2-(2-amino-4-cyanophenylthio)benzylamine
DAT	dopamine transporter
EOS	end of synthesis
FDA	Food and Drug Administration

FPBM	2-(2′-((dimethylamino)methyl)-4′-(3-fluoropropoxy)phenylthio)benzenamine
GP	globus pallidus
HG	Harderian glands
Hp	hippocampus
IACUC	Institutional Animal Care and Use Committee, IPT (*N*-(3′-iodopropen-2′-yl)-2-beta-carbomethoxy-3-beta-(4-chlorophenyl)tropane)
LC	locus coeruleus
(+)-McN5652	trans-1,2,3,5,6,10-beta-hexahydro-6-[4-(methylthio)phenyl-[pyrrolo-[2,1-a]isoquinoline
NC	nasal cavity
OCT	optimal cutting temperature
OT	olfactory tubercle
PCA	p-chloroamphetamine
PET	positron emission tomography
SAIF	small animal imaging facility
SERT	serotonin transporter
SSRI	selective serotonin reuptake inhibitor
St	striatum
Th	thalamus
VMAT2	vesicular monoamine transporter 2

References

[1]. Davidson JR. First-line pharmacotherapy approaches for generalized anxiety disorder. J Clin Psychiatry 2009;70(Suppl 2):25–31. [PubMed: 19371504]

[2]. Nemeroff CB. The burden of severe depression: A review of diagnostic challenges and treatment alternatives. J Psychiatr Res. 2006

[3]. Stafford RS, MacDonald EA, Finkelstein SN. National Patterns of Medication Treatment for Depression, 1987 to 2001. Prim Care Companion J Clin Psychiatry 2001;3:232–35. [PubMed: 15014590]

[4]. Thase ME. Are SNRIs More Effective than SSRIs? A Review of the Current State of the Controversy. Psychopharmacol Bull 2008;41:58–85. [PubMed: 18668017]

[5]. Zhou Z, Zhen J, Karpowich NK, Law CJ, Reith ME, Wang DN. Antidepressant specificity of serotonin transporter suggested by three LeuT-SSRI structures. Nature structural & molecular biology 2009;16:652–7.

[6]. Kugaya A, Sanacora G, Staley JK, Malison RT, Bozkurt A, Khan S, Anand A, Van Dyck CH, Baldwin RM, Seibyl JP, Charney D, Innis RB. Brain serotonin transporter availability predicts treatment response to selective serotonin reuptake inhibitors. Biol Psychiatry 2004;56:497–502. [PubMed: 15450785]

[7]. Meyer JH, Wilson AA, Sagrati S, Hussey D, Carella A, Potter WZ, Ginovart N, Spencer EP, Cheok A, Houle S. Serotonin transporter occupancy of five selective serotonin reuptake inhibitors at different doses: an [11C]DASB positron emission tomography study. Am J Psychiatry 2004;161:826–35. [PubMed: 15121647]

[8]. Ruhe HG, Booij J, v Weert HC, Reitsma JB, Franssen EJ, Michel MC, Schene AH. Evidence why paroxetine dose escalation is not effective in major depressive disorder: a randomized controlled trial with assessment of serotonin transporter occupancy. Neuropsychopharmacology 2009;34:999–1010. [PubMed: 18830236]

[9]. Albin RL, Koeppe RA, Bohnen NI, Wernette K, Kilbourn MA, Frey KA. Spared caudal brainstem SERT binding in early Parkinson's disease. J Cereb Blood Flow Metab 2008;28:441–4. [PubMed: 18073772]

[10]. Guttman M, Boileau I, Warsh J, Saint-Cyr JA, Ginovart N, McCluskey T, Houle S, Wilson A, Mundo E, Rusjan P, Meyer J, Kish SJ. Brain serotonin transporter binding in non-depressed patients with Parkinson's disease. Eur J Neurol 2007;14:523–8. [PubMed: 17437611]

[11]. Meltzer CC, Smith G, DeKosky ST, Pollock BG, Mathis CA, Moore RY, Kupfer DJ, Reynolds CF III. Serotonin in aging, late-life depression, and Alzheimer's disease: the emerging role of functional imaging. Neuropsychopharmacology 1998;18:407–30. [PubMed: 9571651]

[12]. Thomas AJ, Hendriksen M, Piggott M, Ferrier IN, Perry E, Ince P, O'Brien JT. A study of the serotonin transporter in the prefrontal cortex in late-life depression and Alzheimer's disease with and without depression. Neuropathol Appl Neurobiol 2006;32:296–303. [PubMed: 16640648]

[13]. Caretti V, Stoffers D, Winogrodzka A, Isaias IU, Costantino G, Pezzoli G, Ferrarese C, Antonini A, Wolters EC, Booij J. Loss of thalamic serotonin transporters in early drug-naive Parkinson's disease patients is associated with tremor: an [(123)I]beta-CIT SPECT study. J Neural Transm 2008;115:721–9. [PubMed: 18335163]

[14]. Kerenyi L, Ricaurte GA, Schretlen DJ, McCann U, Varga J, Mathews WB, Ravert HT, Dannals RF, Hilton J, Wong DF, Szabo Z. Positron emission tomography of striatal serotonin transporters in Parkinson disease. Arch Neurol 2003;60:1223–9. [PubMed: 12975287]

[15]. Azmitia EC, Nixon R. Dystrophic serotonergic axons in neurodegenerative diseases. Brain Res 2008;1217C:185–94. [PubMed: 18502405]

[16]. Kish SJ, Tong J, Hornykiewicz O, Rajput A, Chang LJ, Guttman M, Furukawa Y. Preferential loss of serotonin markers in caudate versus putamen in Parkinson's disease. Brain 2008;131:120–31. [PubMed: 17956909]

[17]. Garg S, Thopate SR, Minton RC, Black KW, Lynch AJ, Garg PK. 3-Amino-4-(2-((4-[18F]fluorobenzyl)methylamino)methylphenylsulfanyl)benzonitrile, an F-18 fluorobenzyl analogue of DASB: synthesis, in vitro binding, and *in vivo* biodistribution studies. Bioconjug Chem 2007;18:1612–8. [PubMed: 17705553]

[18]. Huang YY, Huang WS, Chu TC, Shiue CY. An improved synthesis of 4-[18F]-ADAM, a potent serotonin transporter imaging agent. Appl Radiat Isot 2009;67:1063–7. [PubMed: 19339192]

[19]. Jarkas N, Voll RJ, Williams L, Votaw JR, Owens M, Goodman MM. Synthesis and *In vivo* Evaluation of Halogenated N,N-Dimethyl-2-(2′-amino-4′-hydroxymethylphenylthio)benzylamine Derivatives as PET Serotonin Transporter Ligands. J Med Chem 2008;51:271–81. [PubMed: 18085744]

[20]. Ma KH, Huang WS, Kuo YY, Peng CJ, Liou NH, Liu RS, Hwang JJ, Liu JC, Chen HJ, Shiue CY. Validation of 4-[18F]-ADAM as a SERT imaging agent using micro-PET and autoradiography. Neuroimage 2009;45:687–93. [PubMed: 19211037]

[21]. Oya S, Choi SR, Coenen H, Kung HF. New PET Imaging Agent for the Serotonin Transporter: [^{18}F]ACF (2-[(2-Amino-4-chloro-5-fluorophenyl)thio]-N,N-dimethyl-benzenmethanamine). J Med Chem 2002;45:4716–23. [PubMed: 12361398]

[22]. Plisson C, Stehouwer JS, Voll RJ, Howell L, Votaw JR, Owens MJ, Goodman MM. Synthesis and *in vivo* evaluation of fluorine-18 and iodine-123 labeled 2beta-carbo(2-fluoroethoxy)-3beta-(4′-((Z)-2-iodoethenyl)phenyl)nortropane as a candidate serotonin transporter imaging agent. J Med Chem 2007;50:4553–60. [PubMed: 17705359]

[23]. Parhi AK, Wang JL, Oya S, Choi SR, Kung MP, Kung HF. 2-(2′-((Dimethylamino)methyl)-4′-(fluoroalkoxy)-phenylthio)benzenamine Derivatives as Serotonin Transporter Imaging Agents. J Med Chem 2007;50:6673–84. [PubMed: 18052090]

[24]. Wang JL, Parhi AK, Oya S, Lieberman B, Kung MP, Kung HF. 2-(2′-((Dimethylamino)methyl)-4′-(3-[(18)F]fluoropropoxy)-phenylthio)benze namine for positron

emission tomography imaging of serotonin transporters. Nucl Med Biol 2008;35:447–58. [PubMed: 18482682]

[25]. Wang JL, Parhi AK, Oya S, Lieberman B, Kung HF. *In vivo* characterization of a series of 18F-diaryl sulfides (18F-2-(2′-((dimethylamino)methyl)-4′-(fluoroalkoxy)phenylthio)benzenamine) for PET imaging of the serotonin transporter. J Nucl Med 2009;50:1509–17. [PubMed: 19690040]

[26]. Takeuchi Y, Sawada T, Blunt S, Jenner P, Marsden CD. Effects of 6-hydroxydopamine lesions of the nigrostriatal pathway on striatal serotonin innervation in adult rats. Brain Res 1991;562:301–05. [PubMed: 1685345]

[27]. Zhang K, Davids E, Tarazi FI, Baldessarini RJ. Serotonin transporter binding increases in caudate-putamen and nucleus accumbens after neonatal 6-hydroxydopamine lesions in rats: implications for motor hyperactivity. Brain Res Dev Brain Res 2002;137:135–8.

[28]. Stachowiak MK, Bruno JP, Snyder AM, Stricker EM, Zigmond MJ. Apparent sprouting of striatal serotonergic terminals after dopamine-depleting brain lesions in neonatal rats. Brain Res 1984;291:164–7. [PubMed: 6199080]

[29]. Molina-Holgado E, Dewar KM, Descarries L, Reader TA. Altered dopamine and serotonin metabolism in the dopamine-denervated and serotonin-hyperinnervated neostriatum of adult rat after neonatal 6-hydroxydopamine. J Pharmacol Exp Ther 1994;270:713–21. [PubMed: 8071864]

[30]. Luthman J, Bolioli B, Tsutsumi T, Verhofstad A, Jonsson G. Sprouting of striatal serotonin nerve terminals following selective lesions of nigro-striatal dopamine neurons in neonatal rat. Brain Res Bull 1987;19:269–74. [PubMed: 3664282]

[31]. Goswami R, Ponde DE, Kung MP, Hou C, Kilbourn MR, Kung HF. Fluoroalkyl derivatives of dihydrotetrabenazine as positron emission tomography imaging agents targeting vesicular monoamine transporters. Nucl Med Biol 2006;33:685–94. [PubMed: 16934687]

[32]. Kilbourn MR, Hockley B, Lee L, Hou C, Goswami R, Ponde DE, Kung MP, Kung HF. Pharmacokinetics of [(18)F]fluoroalkyl derivatives of dihydrotetrabenazine in rat and monkey brain. Nucl Med Biol 2007;34:233–7. [PubMed: 17383572]

[33]. Kung MP, Hou C, Goswami R, Ponde DE, Kilbourn MR, Kung HF. Characterization of optically resolved 9-fluoropropyl-dihydrotetrabenazine as a potential PET Imaging agent targeting vesicular monoamine transporters. Nucl Med Biol 2007;34:239–46. [PubMed: 17383573]

[34]. Boileau I, Rusjan P, Houle S, Wilkins D, Tong J, Selby P, Guttman M, Saint-Cyr JA, Wilson AA, Kish SJ. Increased vesicular monoamine transporter binding during early abstinence in human methamphetamine users: Is VMAT2 a stable dopamine neuron biomarker? J Neurosci 2008;28:9850–6. [PubMed: 18815269]

[35]. Kung MP, Hou C, Lieberman BP, Oya S, Ponde DE, Blankemeyer E, Skovronsky D, Kilbourn MR, Kung HF. *In vivo* Imaging of {beta}-Cell Mass in Rats Using 18F-FP-(+)-DTBZ: A Potential PET Ligand for Studying Diabetes Mellitus. J Nucl Med 2008;49:1171–76. [PubMed: 18552132]

[36]. Harris PE, Ferrara C, Barba P, Polito T, Freeby M, Maffei A. VMAT2 gene expression and function as it applies to imaging beta-cell mass. J Mol Med 2008;86:5–16. [PubMed: 17665159]

[37]. Saisho Y, Harris PE, Butler AE, Galasso R, Gurlo T, Rizza RA, Butler PC. Relationship between pancreatic vesicular monoamine transporter 2 (VMAT2) and insulin expression in human pancreas. J Mol Histol 2008;39:543–51. [PubMed: 18791800]

[38]. Kung M-P, Essman WD, Frederick D, Meegalla S, Goodman M, Mu M, Lucki I, Kung HF. IPT: a novel iodinated ligand for the CNS dopamine transporter. Synapse 1995;20:316–24. [PubMed: 7482291]

[39]. Choi SR, Hou C, Oya S, Mu M, Kung MP, Siciliano M, Acton PD, Kung HF. Selective in vitro and *in vivo* binding of [(125)I]ADAM to serotonin transporters in rat brain. Synapse 2000;38:403–12. [PubMed: 11044887]

[40]. Wilson AA, Ginovart N, Schmidt M, Meyer JH, Threlkeld PG, Houle S. Novel radiotracers for imaging the serotonin transporter by positron emission tomography: synthesis, radiosynthesis, and in vitro and ex vivo evaluation of ^{11}C-labeled 2-(phenylthio)araalkylamines. J Med Chem 2000;43:3103–10. [PubMed: 10956218]

[41]. Soghomonian JJ, Doucet G, Descarries L. Serotonin innervation in adult rat neostriatum. I. Quantified regional distribution. Brain Res 1987;425:85–100. [PubMed: 2448003]

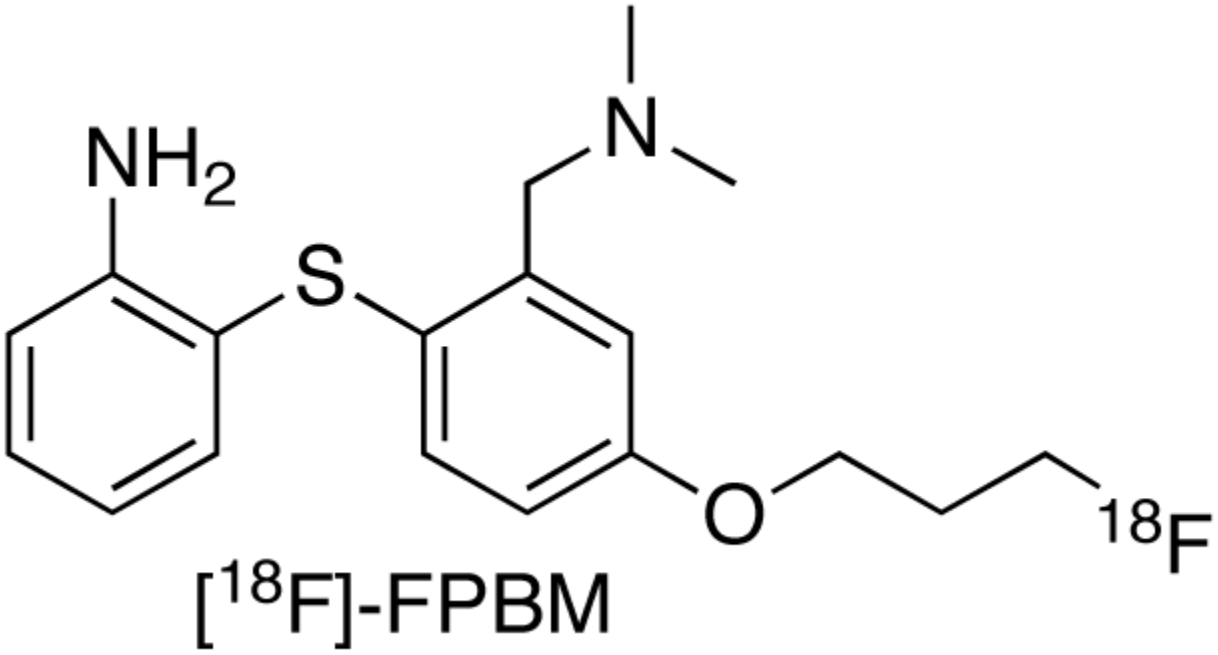

FIGURE 1.
Structure of a potentially new PET radiotracer, [^{18}F]FPBM (2-(2′-((dimethylamino)methyl)-4′-(3-fluoropropoxy)phenylthio)benzenamine), for the imaging of serotonin transporters in the brain.

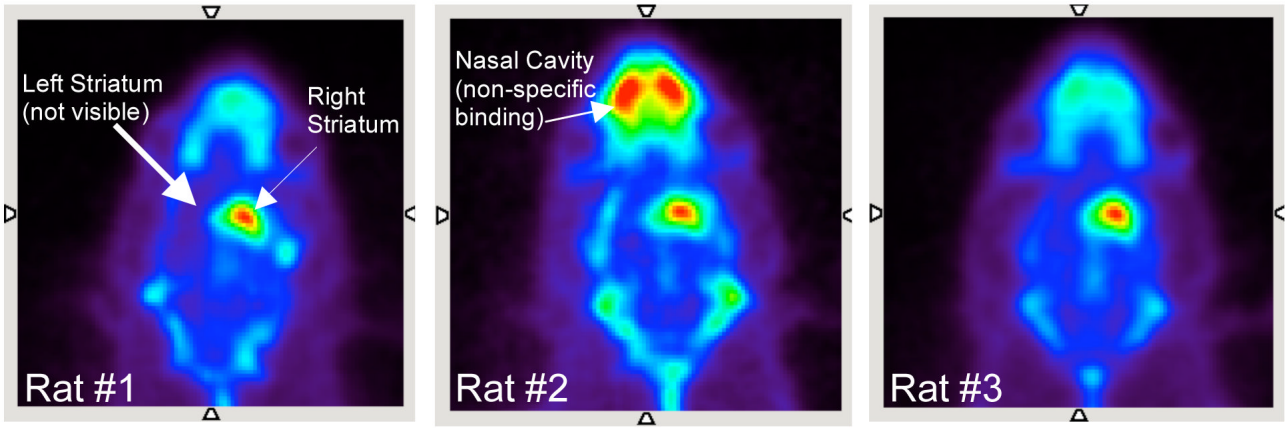

FIGURE 2.

PET imaging was performed to confirm that the 6-hydroxydopamine unilateral lesion of rats #1-3 were successful (n = 1). 50-57 MBq of [^{18}F]AV-133, a VMAT2 ligand, was injected through a catheter placed in the tail vein of the rat while under isoflurane anesthesia. In each of the three rats summed PET images (4 hrs) showed [^{18}F]AV-133 localization to the right striatum but not the left striatum indicating that the lesion was successful. Some non-specific binding can be seen in the nasal cavity.

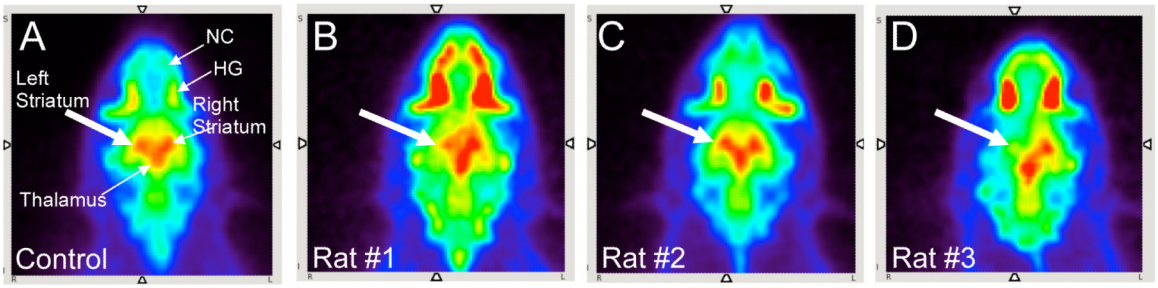

FIGURE 3.

The utility of [^{18}F]FPBM, a SERT ligand, was evaluated in the 6-hydroxydopamine unilateral lesioned rats (rats #1-3) through PET imaging. [^{18}F]FPBM (37-57 MBq), was injected through a catheter placed in the tail vein of the rat while under isoflurane anesthesia. (A) Summed PET images (4 hrs) of a normal control rat showed [^{18}F]FPBM localization to SERT-rich regions such as the thalamus and striatum. (B) In rat #1 there was [^{18}F]FPBM binding in the right striatum but decreased binding in the left striatum (white arrow). (C) In Rat #2 there appeared to be comparable amounts of [^{18}F]FPBM binding between the left (white arrow) and right striatum. (D) There was a clear loss of [^{18}F]FPBM binding in the left striatum (white arrow) of rat #3. Nonspecific binding in the nasal cavity (NC) and Harderian glands (HG) can also be seen in these images.

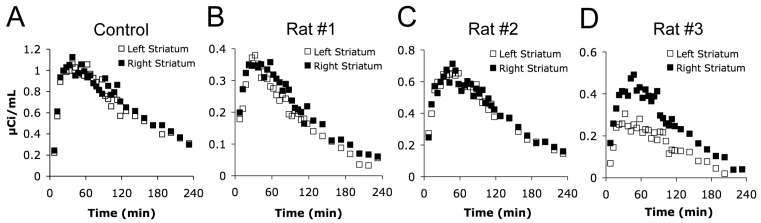

FIGURE 4.

Time activity curves were generated from PET image analysis using the AMIDE software. Points in the curve represent activity in the striatum after subtracting out the activity in the cerebellum at the same time point. Percent [^{18}F]FPBM binding change in the left striatum was expressed as ((total activity in right striatum − total activity in cerebellum) − (total activity in left striatum − total activity in cerebellum))/(total activity in right striatum − total activity in cerebellum) × 100. (A) The normal control rats had a +0.5% average increase in total activity in the left striatum (n = 2, two separate rats). (B) Rat #1 showed an −11% average decrease (n = 2). (C) Rat #2 displayed a −4% average decrease (n = 2). (D) Rat #3 had a −43% average decrease (n = 2).

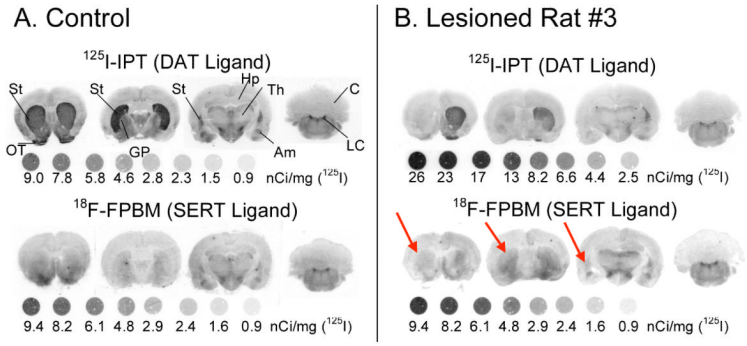

FIGURE 5.

[^{125}I]IPT and [^{18}F]FPBM binding in the striatum of the three Parkinson's model rats were examined through *in vitro* autoradiography. (A) In the control rat, the dopamine transporter ligand, [^{125}I]IPT, strongly binds in both the left and right striatum, as expected. [^{18}F]FPBM also appears to have equal amounts of binding in the left and right striatum. Binding of [^{18}F]FPBM appears less intense than [^{125}I]IPT due to the natural lower level of serotonergic innervation compared to dopaminergic innervation in the striatum. (B) [^{125}I]IPT binding in the left striatum is clearly reduced in rat #3. Rat #3 also had visible differences in [^{18}F]FPBM binding between the left (red arrows) and right striatum. Rat #1 and #2 also showed reduced [^{125}I]IPT binding in the left striatum but did not show any differences with [^{18}F]FPBM (not shown). ^{125}I standards were exposed to the film along with the brain sections. DAT: dopamine transporter, SERT: serotonin transporter, St: striatum, OT: olfactory tubercle, GP: globus pallidus, Hp: hippocampus, Th: thalamus, Am: amygdala, Cb: cerebellum, LC: locus coeruleus (Please note: 1nCi = 0.037 Bq).

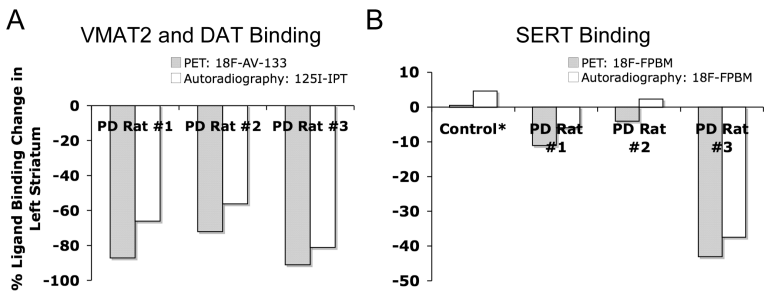

FIGURE 6.

Results from PET imaging and *in vitro* autoradiography show a similar trend. (A) The results from both PET imaging of VMAT2 with [^{18}F]AV-133 and *in vitro* autoradiography of dopamine transporters with [^{125}I]IPT suggest that rat #3 had the greatest loss of dopaminergic neurons followed by rat #1 then rat #2. (B) For *in vitro* autoradiography the percent [^{18}F]FPBM binding reduction was calculated by averaging brain sections containing the rostral striatum (n = 2 for control, n = 3 for rats #1-3). There was variation in values between the brain sections, but the averaged results did rank the rats in the same order of SERT binding loss as the results from PET imaging with [^{18}F]FPBM: rat #3 > rat #1 > rat #2. *Separate control rats were used for PET imaging and *in vitro* autoradiography.

Table 1

Regional Brain Distribution of [^{18}F]FPBM after iv injection of (% dose/gram ± SD)

	PCA Inhibition 60 min (n = 6)	Control 60 min (n = 6)
Cerebellum	0.08 ± 0.01	0.14 ± 0.04
Striatum	0.24 ± 0.07	0.53 ± 0.09
Hippocampus	0.19 ± 0.03	0.45 ± 0.10
Cortex	0.16 ± 0.04[+]	0.49 ± 0.12[+]
Remainder	0.19 ± 0.03	0.45 ± 0.10
Hypothalamus	0.32 ± 0.05[*]	0.66 ± 0.09[*]

Ratio vs. CB ± SD

	PCA Inhibition 60 min (n = 6)	Control 60 min (n = 6)
Cerebellum	1.00 ± 0.34	1.00 ± 0.33
Striatum	2.90 ± 1.00	3.70 ± 1.21
Hippocampus	2.29 ± 0.56	3.09 ± 1.10
Cortex	1.93 ± 0.58	3.39 ± 1.28
Remainder	2.27 ± 0.53	3.12 ± 1.12
Hypothalamus	3.87 ± 0.88	4.61 ± 1.44

[+] Cortex Inhibition: 68% reduction

[*] Hypothalamus Inhibition: 52% reduction